Emerging Microbes & Infections
2026, VOL. 15, 2760628 (12 pages)
https://doi.org/10.1080/22221751.2026.2760628

OPEN ACCESS Check for updates

Nationwide clinical–genomic epidemiology of listeriosis in Taiwan, 2018–2025: disease manifestations in relation to clonal background

Chien-Shun Chiou, Kung-Ching Wang, Jui-Hsien Chang, Hsiao Lun Wei, Yu-Ping Hong, Ying-Shu Liao, You-Wun Wang, Shao-Chun Kuo, Ru-Hsiou Teng and Shiu-Yun Liang

Center for Research, Diagnostics and Vaccine Development, Centers for Disease Control, Ministry of Health and Welfare, Taichung, Taiwan

ABSTRACT

Listeriosis is an uncommon but severe foodborne infection, yet nationwide data linking pathogen genomics with clinical manifestations remain limited. We analyzed 1,252 laboratory-confirmed symptomatic listeriosis cases reported through nationwide surveillance in Taiwan during 2018–2025, with whole-genome sequencing of the corresponding clinical *Listeria monocytogenes* isolate from every case. The average annual incidence was 6.68 cases per 1,000,000 person-years, and 30-day all-cause mortality was 11.4%. Incidence showed an age-dependent sex pattern, with higher incidence among females aged 15–44 years and a shift toward male predominance at older ages. The female excess at ages 15–44 years persisted after exclusion of documented maternal–neonatal cases (male-to-female incidence rate ratio, 0.57; 95% confidence interval, 0.36–0.89). Clonal complex 87 (CC87) was the predominant CC (35.9%), whereas CC1 and CC2 were associated with higher odds of central nervous system (CNS) infection. LIPI-4 occurred predominantly in CC87, and LIPI-4-positive isolates showed lower odds of CNS infection; however, this association could not be separated from clonal background. More broadly, most associations of pathogenicity islands, virulence genes, and their alleles with disease manifestations could not be separated from the underlying clonal backgrounds in which these markers occurred, and none of the estimable associations remained significant after CC adjustment. This nationwide clinical–genomic study characterizes the contemporary burden of listeriosis in Taiwan and highlights clonal background as essential context for interpreting associations between virulence markers and disease manifestations.

ARTICLE HISTORY Received 5 August 2026; Revised 27 October 2026; Accepted 30 October 2026

KEYWORDS *Listeria monocytogenes*; listeriosis; whole-genome sequencing; genomic epidemiology; clonal complex; clinical tropism; LIPI-4; nationwide surveillance

Introduction

Listeria monocytogenes is a foodborne, Gram-positive facultative intracellular pathogen capable of crossing the intestinal, blood–brain, and placental barriers, causing severe manifestations, including bacteremia/sepsis, central nervous system (CNS) infection, and maternal–neonatal disease [1–3]. Although listeriosis is relatively uncommon, it causes substantial morbidity and mortality, particularly among older adults, pregnant women and their fetuses or newborns, and persons with impaired cell-mediated immunity [4]. Despite its relatively low population incidence, the severity of these manifestations makes listeriosis an important foodborne disease. Population-based surveillance is therefore important for defining disease burden, identifying groups at increased risk, and characterizing changes in epidemiology of listeriosis.

Host characteristics strongly influence the epidemiology of listeriosis. Incidence increases markedly with age, pregnancy substantially increases susceptibility among women of reproductive age, and incidence patterns differ by sex and race/ethnicity [5]. Population susceptibility and food exposures may further shape listeriosis burden [6], whereas surveillance and reporting practices influence observed incidence [7]. Circulating *L. monocytogenes* populations vary geographically, with regional differences in clone distributions and source associations [7–9]. In Taiwan, listeriosis became nationally notifiable in January 2018, enabling systematic collection of epidemiological information and clinical isolates for genomic surveillance [7]. An earlier nationwide genomic study covering 2014–2019 documented a marked increase in reported incidence after mandatory notification and identified CC87 as the predominant clinical clonal complex in Taiwan [7]. However, that study included only two years under mandatory notification, limiting characterization of the longer-term population-level burden and epidemiological patterns of listeriosis in Taiwan.

CONTACT Chien-Shun Chiou nipmcsc@cdc.gov.tw; nipmcsc@gmail.com 5F, No. 20, Wen-Sin South Third Road, Taichung City 40855, Taiwan
Supplemental data for this article can be accessed online at https://doi.org/10.1080/22221751.2026.2760628.

© 2026 The Author(s). Published by Informa UK Limited, trading as Taylor & Francis Group, on behalf of Shanghai Shangyixun Cultural Communication Co., Ltd
This is an Open Access article distributed under the terms of the Creative Commons Attribution License (http://creativecommons.org/licenses/by/4.0/), which permits unrestricted use, distribution, and reproduction in any medium, provided the original work is properly cited. The terms on which this article has been published allow the posting of the Accepted Manuscript in a repository by the author(s) or with their consent.

Variation in disease manifestations may reflect not only host characteristics but also heterogeneity within the bacterial population. *L. monocytogenes* has a highly structured clonal population comprising phylogenetically distinct lineages and clonal complexes (CCs) that differ in ecological distribution, virulence-associated genomic features, and association with human disease [9,10]. Integrating human epidemiological and clinical data with bacterial genomics, Maury et al. showed that clinical tropism varies among clones, identified CC1, CC2, CC4, and CC6 as hypervirulent clones, and found that CC1 was associated with CNS infection, whereas CC1, CC2, and CC4 were associated with maternal–neonatal infection [11]. These differences may be related to variation in multiple virulence determinants, including internalins and other factors involved in host-cell invasion and intracellular survival, as well as variation in the *Listeria* pathogenicity islands LIPI-1, LIPI-3, and LIPI-4 [10–12].

Interpretation of genotype–phenotype associations is complicated by the strongly clonal structure of *L. monocytogenes*. Virulence genes, pathogenicity islands, and their allelic variants are often concentrated within lineage-specific genomic backgrounds rather than being broadly distributed across isolates [9,10]. Consequently, an observed association between a virulence marker and a disease manifestation may reflect an association with the marker itself, the genomic background of the lineage carrying it, or both. This distinction is particularly relevant in Taiwan and China, where CC87 is a predominant clinical clone and is commonly associated with LIPI-4 [7,13,14]. By contrast, LIPI-4 was originally identified in CC4 and was experimentally shown, in that clonal background, to contribute to neural and placental tropism [11]. However, the extent to which associations between virulence markers and disease manifestations can be distinguished from effects of the underlying clonal background remains unclear.

In this nationwide clinical–genomic study, we analyzed eight years of surveillance data and whole-genome sequence data from corresponding clinical isolates collected during 2018–2025 to characterize listeriosis incidence, mortality, and demographic and geographic patterns in Taiwan. We further investigated the clonal population structure of clinical *L. monocytogenes* isolates and evaluated associations between disease manifestations and bacterial genomic features, including clonal complexes (CCs), pathogenicity island profiles, virulence genes, and their alleles. A central objective of this study was to determine whether observed associations between virulence-associated genomic markers and disease manifestations could be distinguished from the effects of the underlying clonal background.

Materials and methods

Listeriosis cases, data collection, and bacterial isolates

This nationwide observational study included cases of listeriosis reported to Taiwan's National Notifiable Disease Surveillance System, operated by the Taiwan Centers for Disease Control (Taiwan CDC), between January 2018 and December 2025. The annual numbers of confirmed listeriosis cases are accessible in the Taiwan National Infectious Disease Statistics System (NIDSS; https://nidss.cdc.gov.tw/Home/Index). Demographic, geographic, and clinical data, including age, sex, place of residence, presumed country of exposure, clinical manifestations, and all-cause mortality within 7, 14, 30, and 90 days after disease onset, were obtained from case records in the Taiwan CDC National Infectious Disease Reporting System. The study was approved by the Institutional Review Board of Taiwan CDC (IRB number: 115111).

During the study period, 1,276 cases were recorded in NIDSS. Clinical isolates submitted for these cases were sent to the Central Region Laboratory of Taiwan CDC for species verification and WGS. Cases were excluded if they were reported as asymptomatic or if the submitted isolate was subsequently identified as an organism other than *L. monocytogenes*. Asymptomatic infections had not been systematically excluded from the surveillance database before 2022. The final study population comprised 1,252 laboratory-confirmed symptomatic cases of listeriosis (Table S1). A case was classified as travel-associated when the epidemiological investigation indicated presumed exposure outside Taiwan. When multiple isolates were submitted from the same case, only the first isolate was included in the analysis.

Classification of disease manifestations

Cases were assigned to mutually exclusive disease categories according to clinical manifestations documented in the surveillance records: CNS infection, focal infection, maternal–neonatal infection, and bacteremia/sepsis. Cases with only gastrointestinal or respiratory symptoms, atypical manifestations, or insufficient clinical information to permit assignment to one of these four categories were classified as Others. All 1,252 cases were included in the descriptive epidemiological and incidence analyses. The Others category was clinically heterogeneous and included incompletely characterized cases. Accordingly, the 109 cases in this category were excluded from analyses of associations between bacterial genomic characteristics and disease manifestations, leaving 1,143 cases for these analyses.

Whole-genome sequencing and genomic characterization

Clinical *L. monocytogenes* isolates collected from 2018 to 2024 were subjected to WGS using the Illumina MiSeq platform (Illumina, San Diego, CA, USA), while the isolates collected in 2025 were sequenced using the Oxford Nanopore Technologies (ONT) MinION platform (Oxford Nanopore Technologies, Oxford, UK). Genomic DNA was extracted using the DNeasy Blood & Tissue Kit (cat. no. 69506; Qiagen, Hilden, Germany) according to the manufacturer's instructions.

For Illumina sequencing, libraries were prepared using the Illumina DNA Prep Kit (cat. no. 20018705; Illumina), which involves genomic DNA tagmentation, bead-based cleanup, adapter-indexed PCR amplification, and final purification. Sequencing was performed using a 2×300-bp paired-end configuration, with a minimum sequencing depth of 30× for all isolates. Raw reads were quality-filtered and adapter-trimmed using fastp, and de novo assemblies were generated using SPAdes v4.0.0 [15]. Contigs shorter than 200 bp, with sequencing coverage below 2×, or identified as homopolymer contigs based on sequence complexity assessment were excluded from subsequent analyses. For ONT sequencing, libraries were prepared using the Rapid Barcoding Kit (SQK-RBK114; Oxford Nanopore Technologies) and sequenced on MinION devices equipped with R10.4.1 flow cells (FLO-MIN114). Raw signal data in POD5 format were basecalled using Dorado v1.1.1 with the SUP v5.2.0 model to generate FASTQ reads. De novo long-read assemblies were generated using Flye v2.9.6 and subsequently polished using Medaka v2.0.1. Per-base consensus quality of the polished assemblies was assessed using Alpaqa v0.1.4, which identifies low-quality bases (LQBs; Phred scores 1–5) and quantifies their density per megabase after masking LQB-dense regions. Only assemblies meeting the predefined quality-control criteria were retained for downstream analyses.

WGS-based species identification was performed using Kraken2 v2.1.3 with the PlusPF database (https://benlangmead.github.io/aws-indexes/k2). Sequence types (STs) were assigned using multilocus sequence typing (MLST) v2.25.0 (https://github.com/tseemann/mlst) with the *L. monocytogenes* MLST scheme (listeria_2). Clonal complexes (CCs) and phylogenetic lineages were assigned according to the *L. monocytogenes* nomenclature in BIGSdb-Lm (https://bigsdb.pasteur.fr/listeria/). Sequence-based serogroups and predicted serotype groups were determined using LisSero v0.4.9 (https://github.com/MDU-PHL/LisSero). Pathogenicity islands, virulence genes, and their corresponding alleles were identified using ABRicate v1.0.1 (https://github.com/tseemann/abricate) and a custom database constructed from gene and allele definitions obtained from BIGSdb-Lm (https://bigsdb.pasteur.fr/listeria/), accessed in June 2026. Minimum nucleotide identity and sequence coverage thresholds of 95% and 90%, respectively, were applied for gene identification. LIPI (LIPI-1, LIPI-3, and LIPI-4) types were defined according to the combinations of gene alleles identified among the 1,252 genomes included in the study.

Antimicrobial resistance determinants were identified using AMRFinderPlus v4.0.3 with the National Center for Biotechnology Information (NCBI) AMRFinderPlus database [16]. Plasmid replicon types were identified using PlasmidFinder v2.2.0 and the PlasmidFinder database (https://github.com/genomicepidemiology/plasmidfinder), with minimum nucleotide identity and coverage thresholds of 90% and 60%, respectively.

cgMLST analysis and genetic relatedness

Core-genome multilocus sequence typing (cgMLST) analysis was performed on 1,252 *L. monocytogenes* isolates using an in-house 2,173-locus cgMLST scheme developed by our laboratory. This scheme was established as part of our *L. monocytogenes* genomic surveillance programme and has been routinely applied to isolates collected in Taiwan from different sources, including clinical isolates collected before 2018 and food isolates such as pork and chicken products. In our previous nationwide study [7], the Pasteur cgMLST scheme was used to facilitate comparison with the internationally adopted *L. monocytogenes* cgMLST framework. In the present study, the in-house scheme was retained to provide a consistent analytical framework for the longitudinal Taiwanese clinical collection. Pairwise allelic distances were calculated using loci with valid allele calls in both isolates, with distance defined as the number of loci with discordant allele calls. The resulting pairwise allelic-distance matrix was subjected to single-linkage hierarchical clustering implemented in SciPy [17]. The resulting dendrogram was converted to Newick format and visualized using Interactive Tree of Life (iTOL) v6 [18]. Clonal complexes (CCs), LIPI-3 and LIPI-4 profiles, and clinical manifestations were annotated as metadata tracks. CC/ST groups represented by fewer than 10 isolates were grouped into an "Others" category for visualization.

Statistical analysis

Age was summarized as the median and interquartile range (IQR) and compared across disease categories using the Kruskal–Wallis test. When the overall test was significant, Dunn's pairwise tests were performed with Holm adjustment for multiple comparisons. Sex and 7-, 14-, 30-, and 90-day all-cause mortality were summarized as numbers and percentages and compared

across disease categories using Pearson's chi-square test. Pairwise comparisons were performed only following a significant overall test and were adjusted using the Holm method. CC distributions across disease categories were summarized descriptively as numbers and percentages; formal analyses of associations between CCs and the four major disease categories were conducted separately using Firth logistic regression.

Annual population data for 2018–2025, stratified by age, sex, and city or county, were obtained from the Population Statistics Database of the Department of Household Registration, Ministry of the Interior, Taiwan (https://www.ris.gov.tw/app/portal/346). Annual population counts were summed across the study period to obtain cumulative person-years. Incidence rates were expressed per 1,000,000 person-years with exact Poisson 95% confidence intervals (CIs). Geographic variation in incidence was evaluated using Poisson regression with log person-years as the offset. The overall effect of geographic location was assessed by the likelihood ratio comparison of models adjusted for age group and sex, with and without city or county. For each city or county, a separate Poisson model adjusted for age group and sex compared that location with all other locations combined. Adjusted incidence rate ratios (aIRRs), Wald 95% CIs, and two-sided Wald p values were reported, with Holm adjustment across the 22 location-specific comparisons.

Male-to-female incidence rate ratios (IRRs) with exact conditional Poisson 95% CIs and p values were calculated by age group, with Holm adjustment across the 11 comparisons. Whether the association between sex and incidence varied across age groups was assessed using likelihood-ratio tests of Poisson models with and without a sex-by-age-group interaction, with log person-years as the offset. In a prespecified sensitivity analysis, the 29 female cases classified as maternal–neonatal infection and aged 15–44 years were excluded, and the male-to-female IRR for this age range was recalculated using the same conditional method.

Associations between genomic characteristics and disease manifestations were analyzed among the 1,143 cases in the four major disease categories. Each disease category was compared with the other three using Firth bias-reduced logistic regression, with ORs, 95% CIs, and penalized likelihood ratio p values reported. CCs represented by ≥20 isolates were analyzed individually; less common CCs and ST lineages were pooled as Other CCs. CC19 was used as the reference because its disease distribution approximated that of the overall study population. In a sensitivity analysis, each CC represented by ≥20 isolates was compared with all other CCs combined using the same Firth logistic regression approach. LIPI-1 was analyzed by allelic type, whereas LIPI-3 and LIPI-4 were analyzed by presence or absence and allelic type. LIPI types represented by <20 isolates were pooled as Other types. LIPI-1 type 2 was the reference for LIPI-1 analyses, and absence was the reference for LIPI-3 and LIPI-4 analyses. For type-specific LIPI-3 and LIPI-4 analyses, each type was compared with LIPI-absent isolates, and isolates carrying other types of the same pathogenicity island were excluded from that comparison.

In the broader virulence-marker analysis, genomic variables comprised the LIPI variables described above, presence or absence of individual virulence genes, and virulence-gene alleles. Presence–absence comparisons were performed only when both groups contained ≥20 isolates, and alleles represented by <20 isolates were pooled as Other alleles. For near-universal genes, only allele-based analyses were performed, with the predominant allele among CC19 isolates used as the reference. The same Firth logistic regression framework was applied to each marker contrast for each of the four disease manifestations. Benjamini–Hochberg correction was applied both globally across all marker–outcome comparisons and separately within each disease outcome. Associations between genomic markers and CC were quantified using bias-corrected Cramér's V. Marker–outcome associations with an unadjusted $p < 0.05$ were further evaluated using Firth logistic regression adjusted for CC. Contrasts collinear with CC were classified as not separately estimable, meaning that the effect of the marker could not be distinguished from the effect of the associated CC because the marker distribution was largely determined by clonal background. For estimable contrasts, CC-adjusted ORs, 95% CIs, and p values were reported. The Holm adjustment was applied to the prespecified epidemiological comparison families. All tests were two-sided. Statistical significance was defined as $p < 0.05$ for analyses without multiple-comparison adjustment and as Holm-adjusted $p < 0.05$ or Benjamini–Hochberg-adjusted $q < 0.05$ for the corresponding adjusted analyses. Analyses were performed using Python 3.12.13.

Data availability

The whole-genome sequence data analyzed in this study are available in the NCBI database under BioProject PRJNA493675. BioSample and SRA accession numbers for all 1,252 isolates are listed in Supplementary Table S1.

Results

Clinical characteristics of listeriosis cases

According to the NIDSS, 1,276 listeriosis cases were recorded during 2018–2025. After case verification, 24 were excluded because they were asymptomatic or because the submitted isolate was identified as an organism other than *L. monocytogenes*, leaving 1,252 laboratory-confirmed symptomatic cases. The annual numbers of included cases from 2018 to 2025 were

167, 160, 133, 147, 155, 189, 138, and 163, respectively. Ten cases were travel-associated, with presumed exposure in China (n = 5), Japan (n = 2), Vietnam (n = 2), or Thailand (n = 1). Among the 1,252 cases, 108 (8.6%) were classified as CNS infection, 53 (4.2%) as focal infection, 47 (3.8%) as maternal–neonatal infection, 935 (74.7%) as bacteremia/sepsis, and 109 (8.7%) as Others (Table 1). The 1,143 cases assigned to the four major disease categories were included in subsequent genomic association analyses. The median age was 69 years (IQR, 58.0–79.0), and 608 (48.6%) cases were female. Age and sex differed significantly across disease categories (both $p < 0.001$). Maternal–neonatal cases were significantly younger than cases in all other categories (median, 28 years; IQR, 0.0–34.5) and had a significantly higher proportion of females (85.1%). Overall, 7-, 14-, 30-, and 90-day all-cause mortality rates were 7.7%, 10.0%, 11.4%, and 12.2%, respectively; mortality did not differ significantly across disease categories at any time point (all $p > 0.05$) (Table 1).

Geographic variation in listeriosis incidence

The average annual incidence of listeriosis in Taiwan during 2018–2025 was 6.68 cases per 1,000,000 person-years (95% CI, 6.31–7.06) (Table S2). Crude incidence varied across the 22 cities and counties, ranging from 1.77 to 12.53 cases per 1,000,000 person-years; the highest rates were observed in Hsinchu County (12.53), Chiayi City (10.39), and Taitung County (9.96) (Figure 1; Table S2). Geographic variation in incidence remained significant after adjustment for age group and sex (likelihood-ratio test, $\chi^2 = 88.13$, df = 21, $p < 0.001$). After Holm correction for the 22 location-specific comparisons, Hsinchu County (aIRR, 2.20; 95% CI, 1.69–2.86), Taichung City (aIRR, 1.33; 95% CI, 1.13–1.56), and Taoyuan City (aIRR, 1.34; 95% CI, 1.12–1.60) had significantly higher incidence than all other locations combined (Figure 1; Table S2).

Age- and sex-specific patterns of listeriosis incidence

The association between sex and listeriosis incidence differed significantly by age group (likelihood-ratio test, $\chi^2 = 47.68$, df = 10, $p < 0.001$). Incidence was higher among females at ages 15–44 years, whereas the direction of the sex difference reversed from age 45 years onward, with higher incidence among males (Figure 2; Table S3). After Holm adjustment for the 11 age-group comparisons, significant sex differences remained at ages 25–34 years, with higher incidence among females (male-to-female IRR, 0.27; 95% CI, 0.12–0.54; Holm-adjusted $p = 0.0004$), and at ages 65–74 and 75–84 years, with higher incidence among males (IRR, 1.43; 95% CI, 1.15–1.79; Holm-adjusted $p = 0.0119$; and IRR, 1.54; 95% CI, 1.22–1.95; Holm-adjusted $p = 0.0023$, respectively) (Figure 2; Table S3).

In the sensitivity analysis of persons aged 15–44 years, the higher incidence among females persisted after exclusion of the 29 female cases classified as maternal–neonatal infection in this age range. After exclusion, 56 female and 33 male cases remained, corresponding to incidence rates of 1.52 and 0.86 cases per 1,000,000 person-years, respectively. The male-to-female IRR was 0.57 (95% CI, 0.36–0.89; $p = 0.0106$), indicating that the observed female excess was not explained solely by the documented maternal–neonatal cases.

Population structure, genomic relatedness, antimicrobial resistance determinants, and plasmid replicons

Among the 1,252 clinical *L. monocytogenes* isolates, 812 (64.9%) belonged to phylogenetic lineage I, 437 (34.9%) to lineage II, and 3 (0.2%) to lineage III (Table S1). The isolates comprised 31 CC/ST groups. CC87 was the most common (n = 450, 35.9%), followed by CC19 (n = 205, 16.4%), CC5 (n = 156, 12.5%), CC155 (n = 92, 7.3%), CC1 (n = 75, 6.0%), CC3 (n = 45, 3.6%), CC8 (n = 40, 3.2%), CC101 (n = 37, 3.0%), CC288 (n = 33, 2.6%), and CC2 (n = 28, 2.2%); the remaining groups comprised 91 isolates (7.3%) (Table S4).

cgMLST analysis revealed a highly structured genomic population (Figure 3). Major CCs formed distinct genomic clusters, with the minimum pairwise allelic distance between isolates belonging to different CCs exceeding 800 allelic differences. Several predominant clinical populations, including CC87, CC19/ST378, and ST1081, showed limited within-group diversity. Within-group analyses of CC87 and CC19/ST378 identified multiple closely related isolate groups within a five-allele difference threshold (Figures S1 and S2). ST1081 likewise formed a tightly clustered genomic group.

The distributions of LIPI-3 and LIPI-4 were strongly structured by clonal background. LIPI-3 was distributed across multiple clonal backgrounds, including nine CCs and the ST455 group, whereas LIPI-4 was concentrated predominantly in CC87, with additional occurrences in three less common CCs and the ST455 group (Figure 3). No clear segregation by disease category was apparent in the overall cgMLST clustering pattern, although CNS infections among CC5 isolates were restricted to a single major genomic cluster.

The predominant sequence-based serogroups were IIb (n = 690, 55.1%) and IIa (n = 432, 34.5%), followed by IVb (n = 122, 9.7%) and IIc (n = 5, 0.4%); serogroup

Table 1. Demographic and clinical characteristics of 1,252 laboratory-confirmed symptomatic listeriosis cases by disease category in Taiwan, 2018–2025.

Variable	All, N (%)	CNS infection, N (%)	Focal infection, N (%)	Maternal–neonatal infection, N (%)	Bacteremia/sepsis, N (%)	Others, N (%)
Total N	1,252	108	53	47	935	109
Age, median (IQR)*	69 (58.0–79.0)	66 (55.5–75.3)[a]	71 (62.0–81.0)[ac]	28 (0.0–34.5)[b]	70 (61.0–80.0)[c]	69 (59.0–79.0)[ac]
Female	608 (48.6)	46 (42.6)[a]	23 (43.4)[a]	40 (85.1)[b]	451 (48.2)[a]	48 (44.0)[a]
7-day mortality	97 (7.7)	10 (9.3)	3 (5.7)	1 (2.1)	78 (8.3)	5 (4.6)
14-day mortality	125 (10.0)	12 (11.1)	6 (11.3)	1 (2.1)	101 (10.8)	5 (4.6)
30-day mortality	143 (11.4)	17 (15.7)	6 (11.3)	1 (2.1)	112 (12.0)	7 (6.4)
90-day mortality	153 (12.2)	18 (16.7)	7 (13.2)	1 (2.1)	119 (12.7)	8 (7.3)

Data are presented as N (%) unless otherwise indicated; age is presented as median (IQR). Superscript letters denote post hoc pairwise comparisons for age and sex; values sharing at least one letter did not differ significantly, whereas values with no letter in common differed significantly. Mortality denotes all-cause mortality from disease onset. CNS, central nervous system; IQR, interquartile range.

assignment was unavailable for three isolates. The two predominant predicted serotype groups were 1/2b, 3b, or 7 (n = 690, 55.1%) and 1/2a or 3a (n = 432, 34.5%).

The antimicrobial resistance determinant profile was dominated by *fosX* and *vga(G)*. *fosX* was detected in all isolates, whereas full-length and partial *vga(G)* were detected in 1,232 (98.4%) and 19 (1.5%) isolates, respectively. *tet(M)* was detected in 125 isolates (10.0%), predominantly in CC87 (n = 82) and CC155 (n = 41). Other resistance determinants were rare, with *bla*TEM-116 detected in two isolates and *dfrG* in one. Plasmid replicons were detected in 158 isolates (12.6%), including rep26 in 110 (8.8%), rep25 in 45 (3.6%), and repUS43 in 3 (0.2%).

Clonal complexes and disease manifestations

Among the 1,143 cases assigned to the four major disease categories, associations between CCs and disease manifestations were evaluated using Firth logistic regression, with CC19 as the reference group (Figure 4; Table S5). CC1 (OR, 3.92; 95% CI, 1.71–9.00; $p = 0.0013$), CC2 (OR, 4.76; 95% CI, 1.64–13.80; $p = 0.0073$), and CC5 (OR, 2.23; 95% CI, 1.03–4.82; $p = 0.0384$) showed higher odds of CNS infection than CC19. CC2 (OR, 0.34; 95% CI, 0.14–0.82; $p = 0.0211$) and CC5 (OR, 0.56; 95% CI, 0.32–0.96; $p = 0.0355$) showed lower odds of bacteremia/sepsis. No significant associations were observed between CCs and

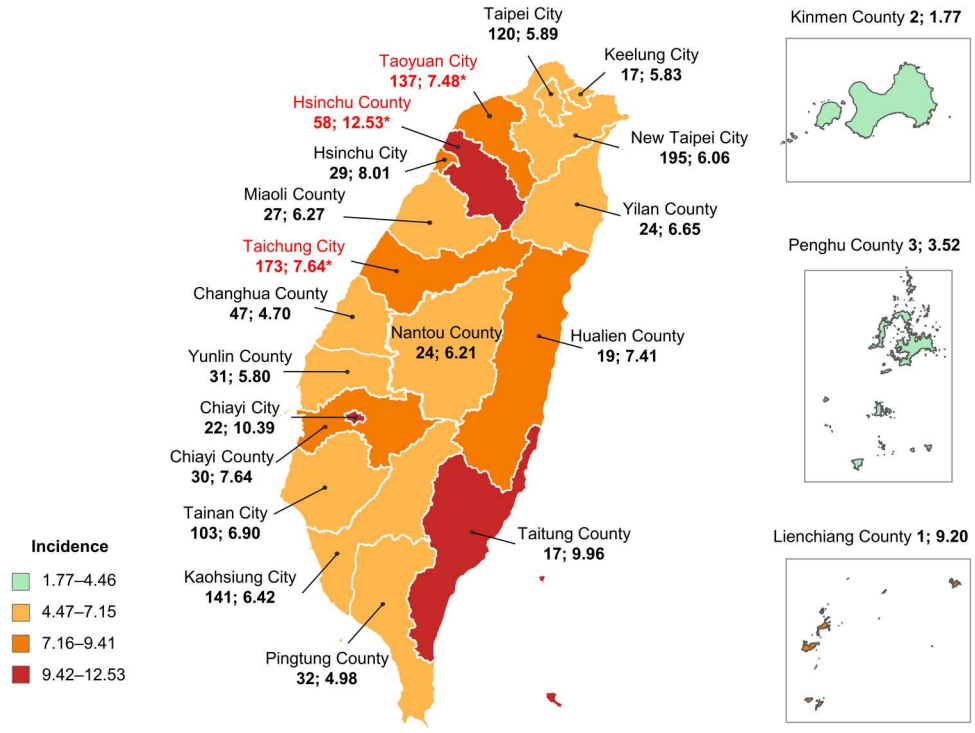


Figure 1. Geographic distribution of listeriosis incidence across cities and counties in Taiwan, 2018–2025. Map shading represents crude incidence per 1,000,000 person-years. Labels show the city or county name, followed by the number of cases and crude incidence, respectively. Asterisks indicate locations with significantly higher age- and sex-adjusted incidence than all other locations combined after Holm correction for multiple comparisons. Detailed estimates are provided in Table S2.

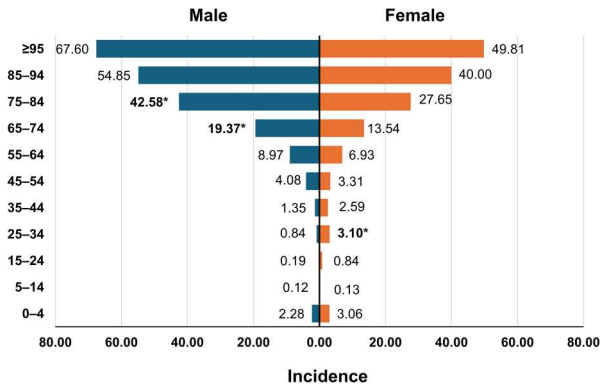


Figure 2. Sex differences in listeriosis incidence across age groups in Taiwan, 2018–2025. Bars show age-specific incidence rates for males and females, expressed as cases per 1,000,000 person-years. Asterisks indicate age groups with a significant difference in incidence between males and females after Holm adjustment for the 11 age-group comparisons. Detailed numbers of cases, male-to-female incidence rate ratios, 95% confidence intervals, and unadjusted and Holm-adjusted *p* values are provided in Table S3.

focal or maternal–neonatal infection (Figure 4; Table S5).

In the sensitivity analysis comparing each CC with all other CCs combined, the higher odds of CNS infection associated with CC1 (OR, 2.71; 95% CI, 1.46–5.02; $p = 0.0034$) and CC2 (OR, 3.14; 95% CI, 1.27–7.77; $p = 0.0249$) remained significant, whereas the association between CC5 and CNS infection was no longer significant (OR, 1.50; 95% CI, 0.88–2.55; $p = 0.1529$). In this alternative comparison, CC87 showed lower odds of CNS infection (OR, 0.64; 95% CI, 0.41–0.99; $p = 0.0393$). The lower odds of bacteremia/sepsis associated with CC2 (OR, 0.40; 95% CI, 0.18–0.89; $p = 0.0345$) and CC5 (OR, 0.63; 95% CI, 0.42–0.96; $p = 0.0357$) also remained significant (Table S6).

Pathogenicity island profiles and disease manifestations

In unadjusted Firth logistic regression analyses, using LIPI-1 type 2, which corresponded to CC19 in this dataset, as the reference, LIPI-1 type 5 (OR, 4.06; 95% CI, 1.68–9.82; $p = 0.0024$) and type 8 (OR, 4.46; 95% CI, 1.45–13.72; $p = 0.0156$) showed higher odds of CNS infection (Table 2). LIPI-1 type 5 occurred exclusively in CC1 and type 8 exclusively in CC2. No LIPI-1 types showed significant associations with focal infection, maternal–neonatal infection, or bacteremia/sepsis.

Compared with LIPI-3-absent isolates, LIPI-3-positive isolates showed higher odds of CNS infection (OR, 1.77; 95% CI, 1.06–2.84; $p = 0.0292$) and lower odds of maternal–neonatal infection (OR, 0.32; 95% CI, 0.07–0.96; $p = 0.0400$). Among the individual LIPI-3 types, type 1 showed higher odds of CNS infection (OR, 2.74; 95% CI, 1.43–4.97; $p = 0.0033$). LIPI-3 was present in 162 isolates spanning nine CCs and the ST455 lineage, whereas all LIPI-3 type 1 isolates belonged to CC1 (Table 2; Table S1).

LIPI-4-positive isolates showed lower odds of CNS infection than LIPI-4-absent isolates (OR, 0.62; 95% CI, 0.39–0.95; $p = 0.0294$), with a similar result for LIPI-4 type 1 (OR, 0.61; 95% CI, 0.38–0.95; $p = 0.0273$) (Table 2). LIPI-4 was present in 416 isolates spanning four CCs and the ST455 lineage; 410 of these isolates (98.6%) belonged to CC87. All LIPI-4 type 1 isolates belonged to CC87 (Table S1).

Virulence-marker associations with disease manifestations in relation to clonal-complex structure

In the broader virulence-marker analysis, 536 nonreference marker contrasts were each evaluated against the four major disease outcomes, yielding 2,144 crude marker–outcome comparisons. Of these, 197 had an unadjusted p value < 0.05, most involving CNS infection (n = 138) (Table S7). After Benjamini–Hochberg correction within each disease outcome, 60 marker–outcome associations remained significant, all involving CNS infection. However, none remained significant when the correction was applied globally across all 2,144 comparisons. Most nominal associations also showed strong dependence on clonal background: 162 of the 197 associations with unadjusted $p < 0.05$ were not separately estimable from CC, and none of the remaining 35 estimable associations retained $p < 0.05$ after CC adjustment (Table S7).

Discussion

This nationwide clinical–genomic study provides a comprehensive characterization of contemporary listeriosis epidemiology in Taiwan, integrating population-level surveillance with genomic analysis of clinical *L. monocytogenes* isolates. Our findings highlight that, beyond demographic and geographic variation in disease incidence, clinical manifestations were strongly associated with clonal background, underscoring the importance of interpreting virulence-associated genomic markers within their lineage-specific contexts.

The average annual incidence of listeriosis in Taiwan during 2018–2025 was 6.68 cases per 1,000,000 person-years, similar to rates reported for the European Union in 2024 (6.9 per 1,000,000) and New Zealand in 2024 (7.0 per 1,000,000), but higher than those reported from U.S. FoodNet sites in 2023 (3.0 per 1,000,000), Canada in 2022 (4.7 per 1,000,000), and Australia during 2016–2023 (2.0–4.0 per 1,000,000) [19–23]. However, these comparisons should be

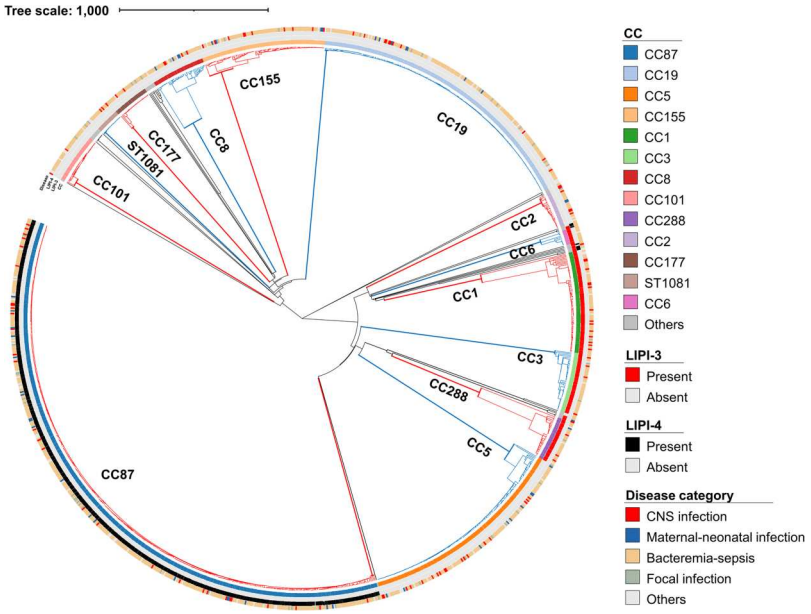


Figure 3. cgMLST-based clustering of 1,252 clinical *Listeria monocytogenes* isolates collected in Taiwan, 2018–2025. A hierarchical clustering dendrogram was constructed based on pairwise allelic distances derived from an in-house 2,173-locus cgMLST scheme. The tree was generated using the single-linkage clustering algorithm and visualized in a circular layout. The outer annotation rings indicate clonal complexes (CCs), LIPI-3 and LIPI-4 profiles, and disease categories. CC/ST groups represented by fewer than 10 isolates were grouped into "Others" for visualization. The scale bar represents 1,000 allelic differences.

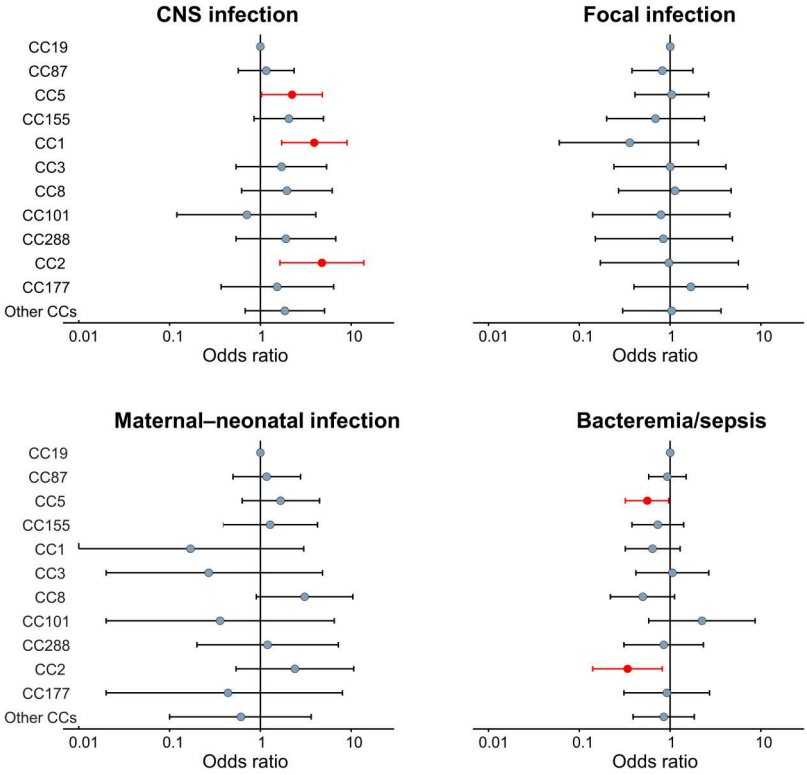


Figure 4. Associations between clonal complexes and disease categories among listeriosis cases in Taiwan, 2018–2025. Forest plots show odds ratios (ORs) and 95% confidence intervals (CIs) for associations between clonal complexes (CCs) and CNS infection, focal infection, maternal–neonatal infection, and bacteremia/sepsis, estimated using Firth bias-reduced logistic regression. CC19 served as the reference group. ORs are plotted on a logarithmic scale. ORs > 1 indicate higher odds and ORs < 1 indicate lower odds of the respective disease category relative to CC19. The vertical line at OR = 1 indicates no association. Red estimates indicate associations with 95% CIs that exclude the null value of 1. The "Other CCs" category comprised CCs and ST lineages represented by fewer than 20 isolates. Detailed estimates and *p* values are provided in Table S5. CC, clonal complex; CI, confidence interval; CNS, central nervous system; OR, odds ratio; ST, sequence type.

Table 2. Associations between LIPI-1, LIPI-3, and LIPI-4 profiles and disease manifestations among listeriosis cases in Taiwan, 2018–2025.

LIPI profile (N)	CNS infection N; OR (95% CI); *p*	Focal infection N; OR (95% CI); *p*	Maternal–neonatal infection N; OR (95% CI); *p*	Bacteremia/sepsis N; OR (95% CI); *p*
LIPI-1 (reference: type 2, N = 183)				
Type 2 (183)	11; 1.00 (reference); –	10; 1.00 (reference); –	7; 1.00 (reference); –	155; 1.00 (reference); –
Type 1 (402)	29; 1.18 (0.59–2.40); 0.6338	19; 0.84 (0.39–1.82); 0.6608	19; 1.20 (0.51–2.83); 0.6792	335; 0.91 (0.57–1.47); 0.7006
Type 3 (139)	17; 2.14 (0.98–4.67); 0.0521	8; 1.07 (0.42–2.71); 0.8900	8; 1.52 (0.56–4.17); 0.4141	106; 0.58 (0.33–1.02); 0.0568
Type 4 (65)	7; 1.92 (0.73–5.06); 0.1956	3; 0.93 (0.27–3.21); 0.9021	4; 1.72 (0.52–5.74); 0.3880	51; 0.65 (0.32–1.32); 0.2409
Type 5 (53)	**11; 4.06 (1.68–9.82); 0.0024**	1; 0.47 (0.08–2.69); 0.3569	0; 0.22 (0.01–3.91); 0.1996	41; 0.61 (0.29–1.29); 0.2022
Type 6 (43)	4; 1.71 (0.54–5.36); 0.3751	2; 1.00 (0.24–4.12); 0.9949	0; 0.27 (0.02–4.83); 0.2831	37; 1.06 (0.42–2.66); 0.9054
Type 7 (32)	1; 0.71 (0.12–4.08); 0.6942	1; 0.79 (0.14–4.54); 0.7830	0; 0.36 (0.02–6.50); 0.4251	30; 2.24 (0.58–8.62); 0.2005
Type 8 (23)	**5; 4.46 (1.45–13.72); 0.0156**	1; 1.10 (0.19–6.44); 0.9154	0; 0.50 (0.03–9.05); 0.6056	17; 0.49 (0.18–1.32); 0.1771
Type 9 (25)	2; 1.60 (0.38–6.70); 0.5404	2; 1.76 (0.41–7.46); 0.4667	0; 0.46 (0.03–8.33); 0.5588	21; 0.88 (0.29–2.61); 0.8136
Other types (178)	21; 2.05 (0.97–4.33); 0.0547	6; 0.62 (0.23–1.69); 0.3471	9; 1.32 (0.49–3.52); 0.5785	142; 0.72 (0.42–1.23); 0.2229
LIPI-3 (reference: absence, N = 981)				
LIPI-3 (162)	**23; 1.77 (1.06–2.84); 0.0292**	4; 0.53 (0.17–1.28); 0.1743	**2; 0.32 (0.07–0.96); 0.0400**	133; 1.01 (0.67–1.58); 0.9558
Type 1 (69)	**14; 2.74 (1.43–4.97); 0.0033**	1; 0.41 (0.05–1.56); 0.2254	0; 0.15 (0.00–1.05); 0.0591	54; 0.79 (0.45–1.46); 0.4315
Type 2 (42)	3; 0.93 (0.25–2.49); 0.8962	2; 1.16 (0.23–3.59); 0.8247	0; 0.24 (0.00–1.75); 0.2050	37; 1.53 (0.67–4.25); 0.3398
Type 3 (31)	4; 1.72 (0.54–4.34); 0.3289	1; 0.93 (0.10–3.63); 0.9275	2; 1.74 (0.35–5.51); 0.4428	24; 0.73 (0.33–1.80); 0.4726
Other types (20)	2; 1.42 (0.28–4.58); 0.6248	0; 0.46 (0.00–3.42); 0.5397	0; 0.50 (0.00–3.75); 0.5926	18; 1.66 (0.52–8.33); 0.4300
LIPI-4 (reference: absence, N = 727)				
LIPI-4 (416)	**29; 0.62 (0.39–0.95); 0.0294**	19; 0.99 (0.55–1.72); 0.9615	19; 1.20 (0.66–2.16); 0.5391	349; 1.25 (0.91–1.73); 0.1678
Type 1 (394)	**27; 0.61 (0.38–0.95); 0.0273**	18; 0.99 (0.54–1.74); 0.9666	19; 1.27 (0.70–2.28); 0.4235	330; 1.24 (0.90–1.72); 0.1956
Other types (22)	2; 0.99 (0.20–3.19); 0.9939	1; 1.40 (0.15–5.72); 0.7076	0; 0.55 (0.00–4.12); 0.6436	19; 1.34 (0.48–5.13); 0.6035

Reference groups were LIPI-1 type 2 for LIPI-1 type comparisons and absence for LIPI-3 and LIPI-4 presence and type comparisons. Other types represent a pooled category of less common types. *p* values are unadjusted. CI, confidence interval; CNS, central nervous system; LIPI, *Listeria* pathogenicity island; OR, odds ratio.

interpreted cautiously because surveillance systems and case definitions differ across countries.

All-cause mortality was 7.7%, 10.0%, 11.4%, and 12.2% at 7, 14, 30, and 90 days, respectively, with little additional increase after 30 days. These estimates were lower than those reported in previous hospital-based studies in Taiwan, including 27.9% mortality within 14 days among patients with bacteremia and 25.2% within 30 days among non-perinatal cases [24,25]. International estimates also vary substantially: a nationwide Danish study reported 27% 30-day mortality among non-pregnancy-associated invasive cases, whereas New Zealand surveillance reported listeriosis-attributed deaths in 11% of non-pregnancy-associated cases with known outcomes; the EU case-fatality rate among cases with known outcomes was 15.6% in 2024 [19,26,27]. However, differences in study populations, inclusion of pregnancy-associated cases, attribution of death, and follow-up periods limit direct comparisons. Thus, our estimates represent fixed-time all-cause mortality among nationally notified symptomatic cases and should not be interpreted as evidence of lower disease severity in Taiwan.

The sex difference in listeriosis incidence varied by age, with higher incidence among females aged 15–44 years and a shift toward male predominance from age 45 years onward. Among persons aged 15–44 years, the female excess persisted after exclusion of the 29 documented maternal–neonatal cases (male-to-female IRR, 0.57; 95% CI, 0.36–0.89). EU/EEA surveillance in 2023 showed a similar age-specific sex pattern: notification rates were higher among females aged 15–44 years but higher among males aged 45 years onward [28]. German nationwide surveillance likewise showed a slight female predominance at ages 18–44 years after pregnancy-associated cases were excluded, followed by male predominance from age 45 years onward [29].

Previous U.S. FoodNet studies estimated that the risk of listeriosis during pregnancy was 91- to 115-fold higher than that among nonpregnant women of similar age, indicating that pregnancy is an important contributor to the higher incidence observed among women of reproductive age [5,30]. Although the female excess at ages 15–44 years persisted after exclusion of the 29 documented maternal–neonatal cases, pregnancy status was not systematically recorded; therefore, pregnancy-associated invasive infections without documented maternal–neonatal outcomes could not be excluded. Unmeasured host and exposure factors, including immunocompromising conditions, medication use, and food exposures, may also have contributed [31,32]. Thus, the factors underlying the residual female excess remain uncertain.

CC1 and CC2 showed higher odds of CNS infection both when compared with CC19 and with all other CCs combined, whereas the CC5 association was observed only when CC19 was the reference (Tables S5 and S6). CC2 and CC5 also showed lower odds of bacteremia/sepsis in both analyses. Because disease categories were mutually exclusive, these latter associations likely reflect differences in the distribution of clinical manifestations rather than reduced ability to cause bacteremia or sepsis. The associations of CC1 and CC2 with CNS infection are consistent with previous evidence of clone-specific clinical tropism and the hypervirulent lineages described by Maury et al. [11], supporting an important role of clonal background in disease manifestation.

In contrast, no significant association was observed between CCs and maternal–neonatal infection, differing from Maury et al., who reported associations with CC1, CC2, and CC4 [11]. The small number of maternal–neonatal cases (n = 47) may have limited statistical power, while differences in population structure, case composition, or epidemiological context may also explain the discrepancy. Thus, the absence of a significant association in the present study should not be interpreted as evidence against the clinical tropism reported previously, but rather as a finding that warrants further investigation in larger cohorts.

LIPI-4 illustrates the importance of clonal context. Maury et al. identified LIPI-4 as a CC4-associated locus and demonstrated its contribution to neural and placental tropism in a CC4 background [11]. In Taiwan, however, LIPI-4 occurred almost exclusively in CC87, and LIPI-4-positive and type 1 isolates showed lower odds of CNS infection (Table 2). CC87 also showed lower odds of CNS infection than all other CCs combined, although not when compared with CC19 (Table S6). The near confinement of LIPI-4 to CC87, together with this reference-dependent CC87 association, makes it difficult to attribute the lower odds of CNS infection to LIPI-4 itself. These findings suggest that the LIPI-4 phenotypic effect may depend on clonal genomic background.

The strong relationship between virulence markers and clonal background extended beyond LIPI-4. Of 2,144 marker–outcome comparisons, 197 had an unadjusted $p < 0.05$, mostly involving CNS infection; 60 remained significant after Benjamini–Hochberg correction within each disease outcome, all for CNS infection, but none after global correction across all 2,144 comparisons (Table S7). Of the 197 nominal associations, 162 were not separately estimable from CC, and none of the remaining 35 estimable associations had $p < 0.05$ after CC adjustment. Thus, these marker–disease associations largely could not be distinguished from clonal-background effects and should not be interpreted as independent virulence-marker effects.

Our findings extend the previous nationwide genomic surveillance study by Tsai et al., which analyzed 411 clinical and 82 food isolates collected during 2014–2019, including 333 clinical isolates from 2018 to 2019, and focused primarily on clinical–food genomic relationships [7]. Incidence during the overlapping 2018–2019 period was similar at approximately 7 cases per 1,000,000 person-years; the slightly lower average incidence during 2018–2025 coincided with fewer reported cases during 2020–2022, a period overlapping with the COVID-19 pandemic. Demographic patterns, clinical manifestations, and the predominance of CC87, CC19/ST378, CC5, and CC155 were also broadly similar, suggesting persistence of established clonal populations. Seven-day mortality was lower in the present study (7.7%) than the 11.9% reported previously among nonmaternal–neonatal cases, although the populations are not directly comparable. Direct comparison of genomic clusters between the two studies is also limited by differences in isolate composition and analytical approaches, including the cgMLST schemes used. Tsai et al. [7] used the internationally established Pasteur cgMLST scheme, whereas the present study used an in-house scheme that has been routinely applied in our laboratory for longitudinal genomic surveillance of *L. monocytogenes* in Taiwan. Therefore, cgMLST cluster boundaries and allelic distances from the two studies should not be considered directly equivalent. Nevertheless, the persistence of CC87, CC19/ST378, CC5, and CC155 as predominant clinical populations across the two surveillance periods supports the continued circulation of established clonal lineages in Taiwan. WGS-based outbreak inference requires epidemiological context. During 2018–2025, no listeriosis outbreak was confirmed through national surveillance, although genomic analyses revealed several closely related isolate groups. When closely related cases were identified, available epidemiological information was reviewed, and cases with identified or suspected epidemiological links were referred to the relevant disease-control units for further investigation. However, no shared food source, exposure history, or environmental linkage sufficient to confirm an outbreak or persistent common-source event was established. The prolonged incubation of listeriosis and the extensive clonality of predominant populations such as CC87 and CC19/ST378 can make genetically related but epidemiologically unrelated cases difficult to distinguish (Figures S1 and S2). Accordingly, genomic relatedness alone is insufficient to define an outbreak in these highly clonal populations. Although unrecognized outbreaks cannot be completely excluded, genomic findings should therefore be interpreted together with epidemiological and source-tracing evidence.

This study has several limitations. First, the surveillance case definition changed during the study period, with asymptomatic *L. monocytogenes* detections not systematically excluded before 2022. Although only symptomatic cases were included in the analyses, changes in surveillance ascertainment may have introduced minor temporal heterogeneity and contributed to discrepancies with NIDSS. Second, pregnancy status, underlying immunocompromising conditions, medication exposure, and food exposure were not systematically available. Consequently, unrecognized pregnancy-associated infections may have contributed to the higher incidence among women aged 15–44 years, and other host- and exposure-related factors could not be evaluated. Finally, international comparisons of incidence and mortality are limited by

differences in surveillance systems, case definitions, study populations, and outcome ascertainment.

In conclusion, this nationwide clinical–genomic study characterized contemporary listeriosis epidemiology and population structure in Taiwan and demonstrated that disease manifestations varied by clonal background. LIPI-4 occurred predominantly in CC87, and its apparent association with lower odds of CNS infection could not be separated from this clonal background. More broadly, most virulence-marker associations were not independently estimable from CC, and none of the estimable associations remained significant after CC adjustment. These findings emphasize that virulence-associated loci should be interpreted within their lineage-specific genomic contexts rather than as isolated predictors of disease phenotype.

Acknowledgments

We thank all participating hospitals for providing *L. monocytogenes* isolates used in this study.

Author contributions

CRediT: **Chien-Shun Chiou:** Conceptualization, Data curation, Formal analysis, Funding acquisition, Investigation, Methodology, Project administration, Resources, Software, Supervision, Validation, Visualization, Writing – original draft, Writing – review & editing; **Kung-Ching Wang:** Data curation, Formal analysis, Writing – original draft; **Jui-Hsien Chang:** Data curation, Methodology, Writing – original draft; **Hsiao Lun Wei:** Data curation, Investigation, Methodology, Writing – original draft; **Yu-Ping Hong:** Data curation, Formal analysis; **Ying-Shu Liao:** Data curation, Funding acquisition, Methodology; **You-Wun Wang:** Data curation, Formal analysis, Methodology; **Shao-Chun Kuo:** Data curation, Formal analysis, Methodology; **Ru-Hsiou Teng:** Data curation, Formal analysis, Investigation; **Shiu-Yun Liang:** Data curation, Methodology.

Disclosure statement

No potential conflict of interest was reported by the author(s).

Funding

This work was supported by the Ministry of Health and Welfare, Taiwan, under grants MOHW108-CDC-C-315-112520, MOHW109-CDC-C-315-122415, MOHW110-CDC-C-315-113107, MOHW111-CDC-C-315-123108, MOHW112-CDC-C-315-133116, MOHW113-CDC-C-315-114110, and MOHW114-CDC-C-315-124112.

References

[1] Disson O, Charlier C, Pérot P, et al. Listeriosis. Nat Rev Dis Primers. 2025;11:71. doi:10.1038/s41572-025-00654-x

[2] Koopmans MM, Brouwer MC, Vazquez-Boland JA, et al. Human listeriosis. Clin Microbiol Rev. 2023;36:e0006019. doi:10.1128/cmr.00060-19

[3] Disson O, Lecuit M. Targeting of the central nervous system by *Listeria monocytogenes*. Virulence. 2012;3:213–221. doi:10.4161/viru.19586

[4] Schlech WF. Epidemiology and clinical manifestations of Listeria monocytogenes infection. Microbiol Spectr. 2019;7:(3):GPP3-0014-2018. doi:10.1128/microbiolspec.GPP3-0014-2018

[5] Pohl AM, Pouillot R, Bazaco MC, et al. Differences among incidence rates of invasive listeriosis in the U.S. FoodNet population by age, sex, race/ethnicity, and pregnancy status, 2008-2016. Foodborne Pathog Dis. 2019;16:290–297. doi:10.1089/fpd.2018.2548

[6] Thomas J, Govender N, McCarthy KM, et al. Outbreak of listeriosis in South Africa associated with processed meat. N Engl J Med. 2020;382:632–643. doi:10.1056/NEJMoa1907462

[7] Tsai YH, Moura A, Gu ZQ, et al. Genomic surveillance of *Listeria monocytogenes* in Taiwan, 2014–2019. Microbiol Spectr. 2022;10:e0182522. doi:10.1128/spectrum.01825-22

[8] Lee S, Chen Y, Gorski L, et al. *Listeria monocytogenes* source distribution analysis indicates regional heterogeneity and ecological niche preference among serotype 4b clones. mBio. 2018;9:e00396-18. doi:10.1128/mBio.00396-18

[9] Moura A, Criscuolo A, Pouseele H, et al. Whole genome-based population biology and epidemiological surveillance of *Listeria monocytogenes*. Nat Microbiol. 2016;2:16185. doi:10.1038/nmicrobiol.2016.185

[10] Orsi RH, den Bakker HC, Wiedmann M. *Listeria monocytogenes* lineages: genomics, evolution, ecology, and phenotypic characteristics. Int J Med Microbiol. 2011;301:79–96. doi:10.1016/j.ijmm.2010.05.002

[11] Maury MM, Tsai YH, Charlier C, et al. Uncovering *Listeria monocytogenes* hypervirulence by harnessing its biodiversity. Nat Genet. 2016;48:308–313. doi:10.1038/ng.3501

[12] Wiktorczyk-Kapischke N, Skowron K, Walecka-Zacharska E. Genomic and pathogenicity islands of *Listeria monocytogenes*-overview of selected aspects. Front Mol Biosci. 2023;10:1161486. doi:10.3389/fmolb.2023.1161486

[13] Huang C, Qin X, Xu G, et al. Persisting predominant clinical CC87 *Listeria monocytogenes* in China: evolutionary dynamics and diversification. Emerg Microbes Infect. 2026;15:2688488. doi:10.1080/22221751.2026.2688488

[14] Zhang H, Chen W, Wang J, et al. 10-Year molecular surveillance of *Listeria monocytogenes* using whole-genome sequencing in Shanghai, China, 2009–2019. Front Microbiol. 2020;11:551020. doi:10.3389/fmicb.2020.551020

[15] Bankevich A, Nurk S, Antipov D, et al. SPAdes: a new genome assembly algorithm and its applications to single-cell sequencing. J Comput Biol. 2012;19:455–477. doi:10.1089/cmb.2012.0021

[16] Feldgarden M, Brover V, Gonzalez-Escalona N, et al. AMRFinderplus and the Reference Gene Catalog facilitate examination of the genomic links among antimicrobial resistance, stress response, and virulence. Sci Rep. 2021;11:12728. doi:10.1038/s41598-021-91456-0

[17] Virtanen P, Gommers R, Oliphant TE, et al. Scipy 1.0: fundamental algorithms for scientific computing in Python. Nat Methods. 2020;17:261–272. doi:10.1038/s41592-019-0686-2

[18] Letunic I, Bork P. Interactive Tree of Life (iTOL) v6: recent updates to the phylogenetic tree display and annotation tool. Nucleic Acids Res. 2024;52:W78–W82. doi:10.1093/nar/gkae268

[19] European Food Safety Authority, European Centre for Disease Prevention and Control. The European Union One Health 2024 zoonoses report. EFSA J. 2025;23:e9759. doi:10.2903/j.efsa.2025.9759

[20] Andersson P, Dougall S, Mercoulia K, et al. Effects of decentralized sequencing on national *Listeria monocytogenes* genomic surveillance, Australia, 2016-2023. Emerg Infect Dis. 2025;31:89–97. doi:10.3201/eid3113.241357

[21] New Zealand Institute for Public Health and Forensic Science. Notifiable diseases in New Zealand: annual report 2024. Porirua: New Zealand Institute for Public Health and Forensic Science (PHF Science); 2025.

[22] Public Health Agency of Canada. National Enteric Surveillance Program (NESP) annual summary 2022. Ottawa: Public Health Agency of Canada; 2024.

[23] Shah HJ, Jervis RH, Wymore K, et al. Reported incidence of infections caused by pathogens transmitted commonly through food: impact of increased use of culture-independent diagnostic tests – Foodborne Diseases Active Surveillance Network, 1996–2023. MMWR Morb Mortal Wkly Rep. 2024;73:584–593. doi:10.15585/mmwr.mm7326a1

[24] Huang YT, Kuo YW, Lee MR, et al. Clinical and molecular epidemiology of human listeriosis in Taiwan. Int J Infect Dis. 2021;104:718–724. doi:10.1016/j.ijid.2021.01.056

[25] Huang SL, Chou YT, Hsieh YC, et al. Epidemiology and clinical characteristics of *Listeria monocytogenes* bacteremia in a Taiwanese medical center. J Microbiol Immunol Infect. 2010;43:485–490. doi:10.1016/S1684-1182(10)60075-8

[26] Jensen AK, Bjorkman JT, Ethelberg S, et al. Molecular typing and epidemiology of human listeriosis cases, Denmark, 2002–2012. Emerg Infect Dis. 2016;22:625–633. doi:10.3201/eid2204.150998

[27] Rivas L, Paine S, Dupont PY, et al. Genome typing and epidemiology of human listeriosis in New Zealand, 1999 to 2018. J Clin Microbiol. 2021;59:e0084921. doi:10.1128/JCM.00849-21

[28] European Centre for Disease Prevention and Control (ECDC). Stockholm2025. Listeriosis – Annual Epidemiological Report for; 2023.

[29] Wilking H, Lachmann R, Holzer A, et al. Ongoing high incidence and case-fatality rates for invasive listeriosis, Germany, 2010–2019. Emerg Infect Dis. 2021;27:2485–2488. doi:10.3201/eid2709.210068

[30] Pouillot R, Hoelzer K, Jackson KA, et al. Relative risk of listeriosis in Foodborne Diseases Active Surveillance Network (FoodNet) sites according to age, pregnancy, and ethnicity. Clin Infect Dis. 2012;54(Suppl 5):S405–S410. doi:10.1093/cid/cis269

[31] Goulet V, Hebert M, Hedberg C, et al. Incidence of listeriosis and related mortality among groups at risk of acquiring listeriosis. Clin Infect Dis. 2012;54:652–660. doi:10.1093/cid/cir902

[32] Preussel K, Milde-Busch A, Schmich P, et al. Risk factors for sporadic non-pregnancy associated listeriosis in Germany-immunocompromised patients and frequently consumed ready-to-eat products. PLoS One. 2015;10:e0142986. doi:10.1371/journal.pone.0142986